JOURNAL OF MATERIALS SCIENCE 28 (1993) 4167–4174

Fabrication of engineering ceramics by injection moulding a suspension with optimum powder properties

Part I *Processing and microstructure*

R. E. F. Q. NOGUEIRA, M. J. EDIRISINGHE*, D. T. GAWNE
Department of Materials Technology, Brunel University, Uxbridge, Middlesex, UB8 3PH, UK

A suspension containing a polypropylene-based high-molecular weight organic vehicle and an alumina powder (which best satisfied criteria for successful compounding, compression moulding, removal of organic vehicle and sintering stages, each necessary for the fabrication of the final ceramic shape) was further assessed in this investigation. Test bars were injection moulded from this suspension under various conditions. After removing the organic vehicle, test bars were sintered and the resulting microstructure studied. The mechanical properties of the test bars will be discussed in Part II.

1. Introduction

The demand for engineering ceramic components has been continuously increasing over the past decade and recent forecasts [1, 2] suggest that this trend will continue in the next five years. However, a major factor curbing demand is the problem of mass producing the required shapes to an acceptable reliability. Although many processes are available for fabricating ceramics [3], mass production of complex shapes with high dimensional accuracy is only obtainable by slip casting and injection moulding; the latter process is much faster. In injection moulding, a ceramic powder is dispersed in an organic vehicle by mixing and compounding to enable shaping by injecting into a mould. Subsequently, the organic vehicle is removed, mainly by pyrolysis, before sintering the ceramic body. Intensive research on moulding ceramic materials only started in the mid 1980s [4], although spark-plug insulators were made using this process in the 1940s [5].

Most of the ceramic injection moulding literature discusses the selection of the organic vehicle on an empirical basis, as shown in a recent review [6]. Various types of polypropylene have been successfully used as the major constituent of the organic vehicle in previous investigations [7–10]. Other minor constituents, particularly a small amount of some processing aid which in many instances is stearic acid [11], are also added to the organic vehicle. The effect of the ceramic powder on the injection-moulding process has been largely ignored in the literature and it is only recently that a few investigations have begun to address various aspects of this issue [12–15]. In particular, as the particle size of the ceramic powder decreases, removal of the organic vehicle becomes difficult and more defects are created [14]. However, sintering favours uniform, unagglomerated, fine ceramic-powder particles [16].

In order to establish the best compromise for the above-mentioned situation with respect to ceramic suspensions containing a high-molecular weight organic vehicle, the authors recently [15] prepared several polypropylene-based formulations with different ceramic powders. The composition of the polypropylene-based organic vehicle was identical to that used in the present investigation. Ceramic powders which allowed the preparation of concentrated suspensions (~ 60 vol % ceramic) with a low Fe take up during compounding were compression moulded and subjected to the removal of the organic vehicle. The sinterability of the ceramic powders selected for moulding was also investigated. Thereby, a ceramic powder (A152.SG, from Alcoa Manufacturing (GB) Ltd, Worcester, UK), which allowed removal of the organic vehicle without the creation of macroscopic defects in compression mouldings and also sintered to a high final density, was selected for further investigation. In the research described in this paper, injection mouldings containing this ceramic powder have been produced using different conditions. Injection moulded test bars were sintered after removal of the organic vehicle and the resulting microstructure was evaluated.

2. Experimental details

2.1. Materials

The particle-size distribution and particle shape of the A152.SG alumina powder (specific surface area $9.2\ m^2\ g^{-1}$) used in this investigation are shown in

* Author to whom all correspondence should be addressed.

0022–2461

TABLE I Details of the organic vehicle constituents

Constituent	Source	Density ($kg\ m^{-3}$)	Molecular weight ($\bar{M}_n$)
Grade GY545M isotactic polypropylene	ICI Ltd, Welwyn Garden City. UK	905	31850
Grade MF5[a] atactic polypropylene	APP Chemicals Ltd, Market Drayton, UK	870	2883
Grade MF70 atactic polypropylene	APP Chemicals Ltd, Market Drayton, UK	870	3603
Stearic acid	BDH Chemicals Ltd, Poole, UK	941	Relative molecular mass = 284

[a] Production discontinued during research programme. Grade MF70 used instead in formulations 2 and 3.

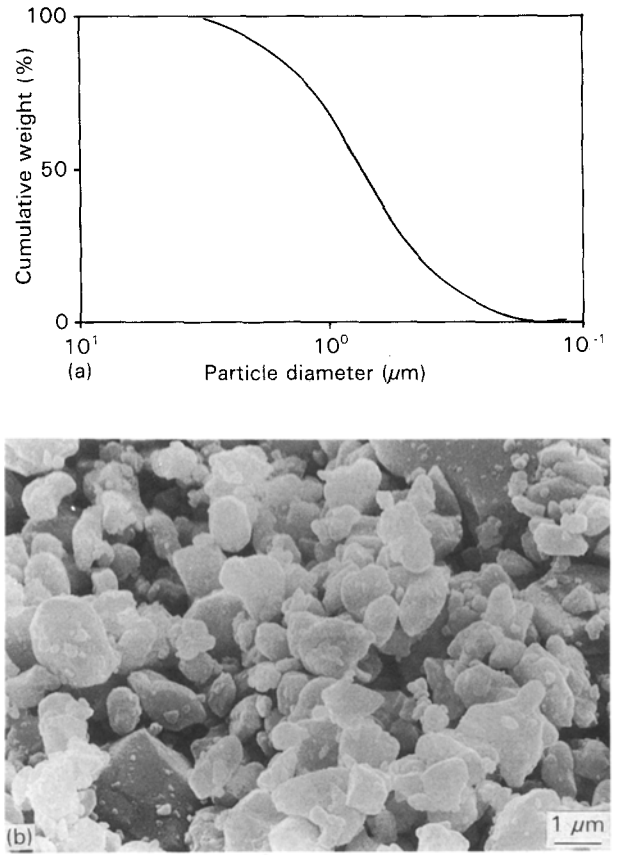

Figure 1 (a) Particle size distribution, and (b) scanning electron micrograph of the alumina powder used.

Fig. 1. Details of the organic vehicle are given in Table I. Isotactic polypropylene, atactic polypropylene and stearic acid were mixed in the weight ratio 4:4:1.

2.2. Mixing and compounding

The ceramic powder was mixed with 0.25 wt % magnesia (a sintering aid) in a ball mill for 3 h at 25 r.p.m. (revs per minute). The powder containing the sintering aid was then mixed with stearic acid in a Henschel high-speed mixer at 3000 r.p.m. for 5 min. Subsequently, polypropylene was added and mixing was continued for another 5 min. Using this method, three 1.5 kg batches of formulation 1 were prepared.

Similar batches of formulations 2 and 3 were also prepared with changes in the mixing procedure. In the case of formulation 2, stearic acid was mixed with the ball-milled ceramic powder (same conditions as for formulation 1) by tumbling in a container for approximately 5 min. This was followed by addition of the polymers and tumbling was continued for a further 5 min. The ceramic powder used to prepare formulation 3 was dried in a vacuum oven at 100 °C before being milled with the sintering aid (same conditions as in formulation 1). Stearic acid was then added by mixing in the Henschel high-speed mixer at 3000 r.p.m. for 5 min. The polypropylene was mixed in by tumbling in a container for approximately 5 min.

TABLE II Compounding conditions

Screw diameter (mm)	40
Screw length/dia. ratio	17
Screw speed (r.p.m.)	60
Barrel temperature profile (Feed to Exit, °C)	180–180–190–190

The three batches of each formulation were compounded using a co-rotating, intermeshing twin-screw extruder (from Betol Machinery, Luton, UK) under the conditions given in Table II. Details of the extruder and the procedure, which enables the preparation of well-dispersed concentrated suspensions containing high-molecular weight polymeric organic vehicles, have been fully discussed previously [9, 17, 18]. The extrudate was cooled in water and dried in a vacuum oven at 60 °C for 24 h. The dried extrudate was granulated. In the case of formulation 3, the dried and granulated extrudate was re-extruded. Four samples (~3 g) of each formulation were ashed by heating to 600 °C in order to estimate the exact volume percentage of ceramic present.

2.3. Injection moulding

Tensile test bars, 190 mm long and 3 mm thick, were produced from all three formulations by injection moulding the granulated material using a Sandretto 6GV/50 reciprocating-screw machine. A single-gated test-bar mould was used, which allowed the production of two tensile test bars each time the material was injected. The injection moulding conditions are given in Table III. Test bars were produced from formulation 1 using various injection pressures (in the range 38–109 MPa). Test bars from formulations 2 and 3 were produced with injection pressures of 83 and 127 MPa, respectively.

The ends (50 × 19 × 3 mm) of the as-moulded tensile test bars (Fig. 2) were removed and some of these were used as the specimens for the ashing experiments

TABLE III Injection moulding conditions

Dose (cm^3)	46
Total injection time (s)	16
Barrel temperature (°C)	
supply zone	190
middle zone	210
forward zone	230
nozzle	235
Mould temperature (°C)	55

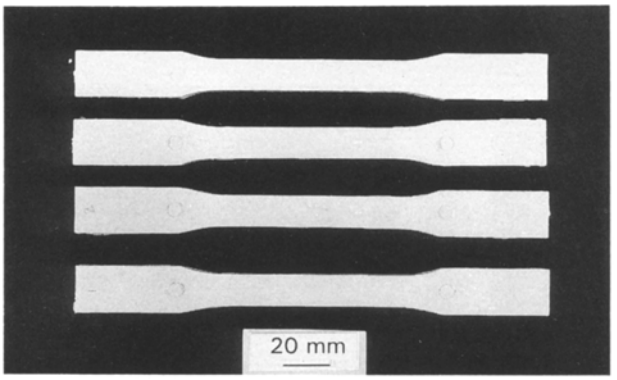

Figure 2 As-moulded tensile test bars.

described below. Three specimens, each representing different test bars, from each formulation were sectioned into five equal parts along their length in the direction perpendicular to their cross-section. The resulting samples (five from each moulding) were ashed by heating to 600 °C.

The central rectangular region (approximately $72 \times 13 \times 3$ mm) of each test bar was used for experiments on removal of the organic vehicle and sintering. Prior to these experiments, bars were contact-radiographed using a Hewlett Packard Faxitron X-ray system operating at 30 kV and 3 mA with an exposure time of 3 min to determine the presence of macroscopic defects.

2.4. Removal of organic vehicle

Shavings from the mouldings of all three formulations were heated in a Perkin-Elmer TGS-2 thermobalance in flowing air (at a flow rate of approximately 60 $mm^3 s^{-1}$). The heating rate was 5 °C min^{-1}.

A chamber furnace (model SHFC, from Lenton Thermal Designs Ltd, Market Harborough, UK) was used to heat the test bars in static air in order to remove the organic vehicle. The temperature in the furnace was controlled by a 818P Eurotherm programmer. Heating from room temperature to 150 °C, which is approximately the softening point of the formulation, was done at 60 °C h^{-1} followed by soaking at this temperature for 24 h. Heating was then continued at 2 °C h^{-1} to either 350 °C (ramp 1), 250 °C (ramp 2) or 200 °C (ramp 3) when the mouldings were subjected to a soak time of 24 h. The final phase of heating to 450 °C was carried out at 2 °C h^{-1} followed by cooling in the furnace to room temperature. The test bars were supported by an alumina powder bed contained in an aluminium tray. Test bars of formulations 1 and 2 were X-ray radiographed after removal of the organic vehicle using the system and conditions mentioned in Section 2.3 in order to detect macroscopic defects. In the case of formulation 3, test bars were sintered after removal of the organic vehicle and their cross-sections were examined using microscopy as described below.

2.5. Sintering

After removal of the organic vehicle, test bars of formulation 3 (and a few of formulation 1) were sintered in static air in a chamber furnace (model LTD1700, from Lenton Thermal Designs Ltd, Market Harborough, UK) by heating to 1650 °C at 30 °C per minute and soaking at this temperature for 2 h. Subsequently, the test bars were cooled in the furnace to room temperature. The densities of thirty sintered specimens (numbers 1–30) of formulation 3 was measured using mercury immersion [19]. These sintered test bars were used for mechanical and wear tests and the results will be described in Part II.

2.6. Microstructure

Specimens representative of the cross-section of sintered test bars of formulation 3 were cut from a region a few millimetres below the fracture surface resulting from flexural testing. These were mounted in cold resin and ground on a flat glass plate using SiC powder (170, 30, 20 and 12 μm grits were used in that order) before polishing with 6 and 1 μm diamond paste. The cross-sections were examined for microscopic defects using a Cambridge S250 scanning electron microscope. Nine test bars (numbers 1, 7, 13, 17, 18, 25–27 and 29) were investigated in this manner.

The surface (35×13 mm) of three specimens (halves of test-bar numbers 8, 11 and 20 resulting from flexure testing) were ground and polished as above and thermally etched (1500 °C for 2 h in air) to reveal the grain structure. Ten regions of each specimen were studied using an optical microscope and the average grain size of each region was measured by a linear intercept method [20, 21]. The specimens were lightly coated with gold to avoid charging before being further examined with the scanning electron microscope.

3. Results and discussion

3.1. Compositions

Table IV shows the weight percentages of ceramic in each formulation, calculated from the ashing results. Using the mean weight percentage of ceramic and assuming that the constituents of the organic vehicle were present in the same ratios in which they were added, the volume percentages of ceramic present in formulations 1, 2 and 3 are 62.0, 59.1 and 62.9, respectively.

TABLE IV Ashing results of the extrudate (wt % ceramic);

Formulation	Ceramic content (wt %)				
	Sample 1	Sample 2	Sample 3	Sample 4	Mean value
1	88.50	87.85	87.79	87.56	87.93 (0.35)[a]
2	86.83	86.86	86.90	85.68	86.57 (0.51)[a]
3	88.24	88.81	88.36	87.95	88.34 (0.31)[a]

[a] Standard deviation

TABLE V Ashing results of test bars (TB) expressed as volume percentages of the ceramic

Sample number	Ceramic content (vol %)								
	Formulation 1			Formulation 2			Formulation 3		
	TB1	TB2	TB3	TB1	TB2	TB3	TB1	TB2	TB3
1	61.7	60.4	63.0	59.7	58.1	59.8	63.7	62.7	63.9
2	60.7	62.2	62.7	59.4	59.1	59.7	63.7	62.8	62.7
3	63.3	61.9	62.9	59.7	59.8	59.3	63.1	62.4	62.0
4	62.5	62.3	61.5	59.6	60.7	59.3	62.4	62.1	62.8
5	62.1	62.0	62.5	60.6	60.3	59.5	63.2	62.6	63.4
Mean value	62.1	61.8	62.5	59.8	59.6	59.5	63.2	62.5	63.0
Standard deviation	0.9	0.7	0.5	0.4	0.9	0.2	0.5	0.3	0.7

3.2. Effect of processing variables

Table V shows the ashing results of the samples taken from mouldings of each formulation. The ceramic content (vol %) is calculated on the basis stated in Section 3.1. The standard deviation of the variation of ceramic content across the cross-section was less than 1 vol % in all three formulations and therefore in this respect variations in the mixing method were not critical. In particular, tumbling in a container was as effective as using a high-speed mixer for the initial mixing stage.

Test bars of formulation 1 were blue coloured after sintering. Trial-and-error experiments revealed that the colour first appeared at 1400 °C during sintering. The colour of alumina artefacts depends on the additives/impurities present and the sintering atmosphere [22]. MgO, which aids densification during sintering by eliminating discontinuous grain growth, thereby helping to produce a fine-grained microstructure [23], could only result in a pale cream or grey colour [22]. The impurity which is most likely to produce the blue colour is Fe, which is taken up due to wear of the machinery during processing. In fact, the presence of Fe_2O_3 is well known as the cause of the blue colour of engineering bricks [24] and magnesium aluminate spinel [25].

Analysis (by inductively-coupled-plasma optical-emission spectroscopy after leaching the Fe into solution using concentrated HCl; performed by MEDAC Ltd, Brunel University, UK) of the Fe in formulations 1, 2 and 3 (Table VI) showed that formulation 1 had a much higher Fe content; the 10 min high-speed mixing before compounding is the reason for this. In fact, after mixing, this blend had a distinct grey colour distinguishing it from the other formulations; this indicates the higher Fe take up. The presence of a transition metal such as Fe also results in catalysis of the oxidative degradation occurring during removal of the organic vehicle [26]. Thermogravimetric traces of the compositions (Fig. 3) show evidence of this as formulation 1 begins to lose the organic vehicle at a lower temperature.

TABLE VI Fe present in each formulation

Formulation	Fe content (p.p.m.)
1	399
2	73
3	152

Fig. 4 shows X-ray radiographs of test bars of formulation 1 moulded using different injection pressures. It shows that an injection pressure of 38 MPa was sufficient to produce test bars free of macroscopic defects. Fine cracks in mouldings usually become extensive only after removal of the organic vehicle. Therefore, defects such as shrinkage-related cracking may be apparent only after removal of the organic vehicle [27]. In fact, radiographs of test bars of formulation 2 made using an injection pressure of 83 MPa did not show any defects in the as-moulded state, but cracking occurred after removal of the organic vehicle (using ramp 2) at the center of the cross-section along the entire length and this virtually separated the test bar into two layers (Fig. 5). This type of cracking was not present in test bars of formulation 1, in which other defects caused by removal of organic vehicle were present as discussed later.

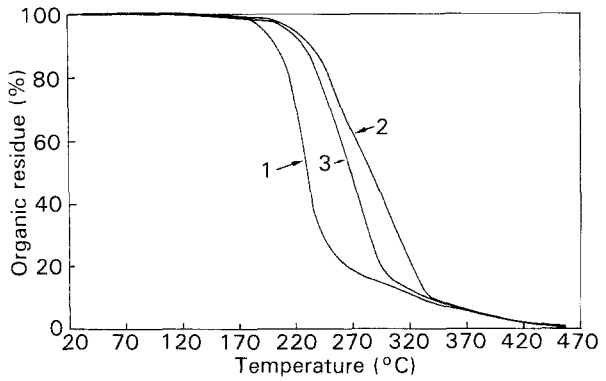

Figure 3 Thermograms of the formulations.

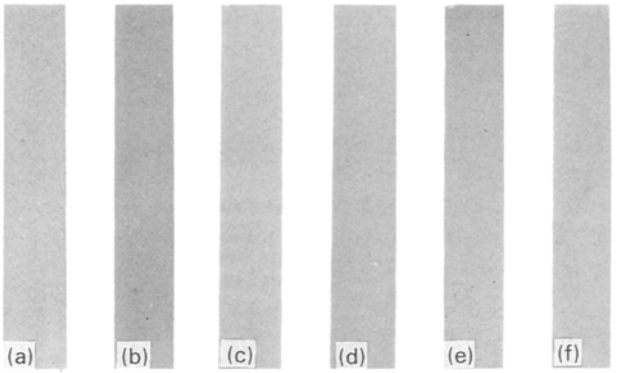

Figure 4 Test bars of formulation 1 moulded using different injection pressures: (a) 38 MPa, (b) 51 MPa, (c) 70 MPa, (d) 90 MPa, (e) 102 MPa, and (f) 109 MPa.

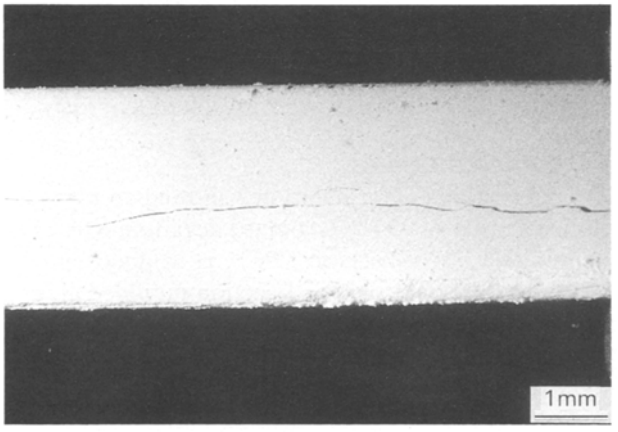

Figure 5 Cracking in test bars of formulation 2 after removal of the organic vehicle.

Ashing results of the top and bottom halves of several test bars (as-moulded) of formulation 2 sectioned at the centre along their lengths are given in Table VII. The ceramic contents (vol %) in each half, calculated on the basis stated in Section 3.1, do not show significant differences. Therefore, the defects are not caused by the differential shrinkage of two different compositions, prevailing in the top and bottom halves of the test bars, during removal of the organic vehicle. The injection pressure of 83 MPa, although

TABLE VII Ashing of test bars (TB) of formulation 2 expressed as vol % of ceramic

	Ceramic content (vol %)					
	TB1	TB2	TB3	TB4	TB5	TB6
Top half	58.3	57.1	58.7	59.0	59.0	59.1
Bottom half	57.8	57.9	58.7	58.5	58.4	58.5

sufficient to prevent voids which are typical defects caused by a low injection pressure [28], seems to be inadequate in preventing cracking in formulation 2 which contains a higher (by 3 vol%) organic-vehicle content than formulation 1. This type of crack at the centre of the test bars can be so fine and shallow across the thickness in the as-moulded state that cracks are not detected by X-ray radiography in the lateral direction. The thickness of test bars is only 3 mm, making it difficult to produce meaningful X-ray radiographs in the longitudinal direction. Microscopic examination of as-moulded, test-bar cross-sections was not useful in revealing these fine cracks; this could be due to the smearing of the polymeric organic vehicle during polishing. This type of cracking was not observed in our previous work [15] where compression mouldings, cylinders of 18 mm diameter and 30 mm length, were made using the same suspension. The organic vehicle in these cylinders was removed by heating in nitrogen. Therefore, a few test bars of formulation 2 were heated in nitrogen according to the same temperature ramp used for the compression mouldings [15]. Cracking similar to that observed in those test bars pyrolysed in air (Fig. 5) was present in the test bars after removal of the organic vehicle. However, this cracking was not as extensive as that found in the test bars pyrolysed in air. X-ray radiographs of these test bars subjected to removal of the organic vehicle in air and nitrogen also show an almost identical pattern of internal defects (Fig. 6). A comparison of ceramic mouldings made using compression and injection moulding is beyond the scope of this investigation but the following comparisons show that several differences exist. The conditions mentioned for compression moulding are those used in our previous work [15].

The compression pressure (12 MPa) was lower than the injection pressure (83 MPa). The compression mouldings solidified in a die cooling slowly from 200 °C to room temperature. For comparison, the injection mouldings solidified in a mould held at 50 °C after injecting the suspension at 230 °C (Table III). These factors will mean that the moulding shrinkage and residual stress in the two types of mouldings will be quite different. Also, the flow of suspension in the mould cavity during compression moulding differs substantially to that prevailing during injection moulding and the resulting arrangement of ceramic particles in the two instances could be quite dissimilar. Differences in geometry in the mouldings will complicate the above comparisons even further. Compression moulding is commonly used in investigations instead of injection moulding because the former

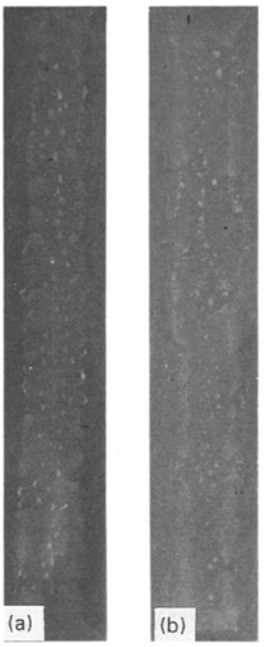

Figure 6 X-ray radiograph of test bars of formulation 2 subjected to removal of the organic vehicle in: (a) air, and (b) nitrogen.

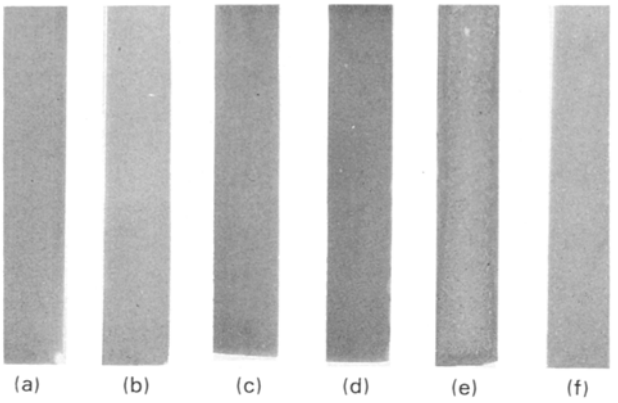

Figure 7 Test bars of formulation 1 after removal of the organic vehicle (the corresponding as-moulded bars are given in Fig. 4). Test bar (e) was pyrolysed according to temperature ramp 1. The other test bars were pyrolysed according to temperature ramp 2. (a) 38 MPa, (b) 51 MPa, (c) 70 MPa, (d) 90 MPa, (e) 102 MPa, and (f) 109 MPa.

method is more feasible for fabricating simple shapes from a small quantity of material. However, the results of this investigation raise the important issue of whether experiments performed using compression mouldings provide information on characteristics of injection mouldings.

The first temperature ramp (soak at 350 °C for 24 h) used to remove the organic vehicle from mouldings of formulation 1 in static air was identical to that used in previous work where mouldings were pyrolysed in nitrogen [14, 15]. However, pyrolysis according to this schedule caused an extensive network of voids and cracks in the test bars, e.g. Fig. 7e. These defects are caused by removal of the organic vehicle and are not related to the injection-moulding stage because test bars made with both lower and higher injection pressures (compared with those used to mould the test bar shown in Fig. 7e) did not contain the same extensive network of defects after pyrolysis (Fig. 7a–d and f) using temperature ramp 2 where the soak temperature was reduced to 250 °C.

Thermogravimetric studies provide the explanation for the above observations. The intention of the soak temperature is to decrease the rate of the major weight loss during the pyrolysis of the mouldings. The temperature ramp with the soak temperature at 350 °C was suitable for removal of the organic vehicle in a nitrogen atmosphere where the major weight loss started at about 350 °C [14]. In air, the major weight loss in fine material of formulation 1 begins at approximately 200 °C (Fig. 3). The thermogravimetric trace representing pyrolysis in air will be displaced to the right-hand side as the cross-section thickness of the sample increases; the reasons for this have been explained previously [29]. Therefore, a soak temperature of 250 °C was more appropriate for the temperature ramp used to pyrolyse mouldings in air. This also shows the importance of the atmosphere in which removal of the organic vehicle takes place. It affects the mechanism by which removal of the organic vehicle occurs [29–31]. In air, oxidative degradation of polypropylene occurs in the surface regions, while thermal degradation occurs in the core of the specimen. Removal of the organic vehicle is therefore accelerated, and with increasing sample thickness degradation is controlled by the rate of diffusion of oxygen into the moulding [32]. In nitrogen only thermal degradation occurs. Since some of the test bars of formulation 1 contained a few fine cracks after the removal of organic vehicle using temperature ramp 2 (Fig.7a–d and f), the soak temperature used during pyrolysis of specimens of formulation 3 was further reduced to 200 °C (ramp 3).

3.3. Sintered bodies

Sintered test bars of formulation 3 showed an average relative density of 95.7% (standard deviation 0.6). The average relative density of ~96% is in good agreement with data published on injection-moulded alumina bodies [33, 34]. In fact, these data [33, 34] refer to specimens made using A16.SG alumina which is usually a powder with a narrower-particle-size distribution and a lower (< 1 μm) median particle size than A152.SG alumina. Such powders have better sinterability [16] and therefore the final density achieved in this investigation is satisfactory, although there is room for improvement as discussed below.

Alumina containing MgO as a sintering aid can be sintered to the theoretical density provided the atmosphere used for firing contains gases that are soluble in alumina and are therefore able to diffuse from closed pores [35, 36]. These specimens were sintered in air and the limited solubility of the nitrogen present causes the relative density to be lower than 98%; it is often in the range 92–96% [36]. Scanning electron micrographs of polished and thermally etched specimens show pores in grains and at grain boundaries due to incomplete densification (Fig. 8).

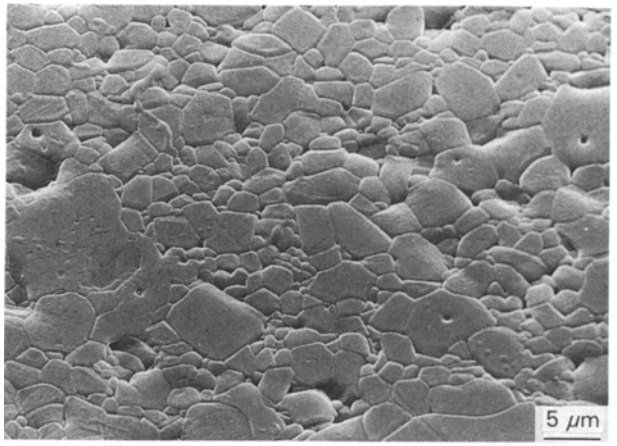

Figure 8 Scanning electron micrograph of a polished specimen (thermally etched) showing the grain structure of a sintered test bar.

Although the alumina powder was selected because it had the optimum particle characteristics to suit the high-molecular weight polymeric organic vehicle and the various stages of the shaping method, further improvements in the particle-size distribution of the powder can be made. It contains particles ranging from ~5 to ~0.1 μm and therefore can be considered as a wide particle-size distribution compared to A16.SG alumina. A wide particle-size distribution helps to achieve more efficient packing [37] but is less favourable for forming final ceramic shapes with a low porosity [38]. Therefore, the particle-size distribution of the alumina used can be further optimized while retaining the median particle size of ~1 μm which especially suits the organic-vehicle removal stage.

Figure 9 Fine pores seen at the centre of the cross-section of a sintered test bar.

TABLE VIII Grain-size measurements; the standard deviation of the average grain sizes, measured in ten areas of each specimen, is given in parentheses

Specimen number	Average grain size (μm)
8	7.5 (0.9)
11	7.5 (0.8)
20	7.2 (0.7)

Microscopical examination of cross-sections of sintered bodies showed that fine pores were present at the centre of several specimens (Fig. 9). These originate during the removal of the organic vehicle and can be eliminated if degradation takes place at a higher temperature at a slower rate. Both these factors help the diffusion of degradation products to the surface; but, as discussed earlier, these conditions cannot be satisfied when pyrolysis is done in air as the presence of oxygen accelerates degradation, and the removal of the organic vehicle takes place at a much lower temperature. This is supported by the fact that a few test bars pyrolysed in nitrogen, according to the temperature ramp used previously [15] and sintered according to the procedure described in Section 2.5, did not show such defects. In nitrogen the major weight loss occurs much later at (~350 °C). Grain-size measurements are shown in Table VIII. They show that the average grain size of the sintered bodies is ~7 μm. The variation of average grain size between different regions in each specimen is extremely small (Table VIII). The technical group (A1–A12) classification [39] of these sintered alumina bodies will be discussed in Part II, together with the mechanical properties.

4. Conclusions

This investigation has shown that the use of sophisticated machinery (e.g. high-speed mixers) for the mixing of the ceramic powder and the constituents of the organic vehicle prior to compounding does not offer any advantages in terms of the homogeneity of the formulation produced. In fact, it could result in the formulation being contaminated with Fe due to wear of the machinery.

The temperature ramp used for the removal of the organic vehicle from injection moulded artefacts should be designed to suit the atmosphere in which pyrolysis is carried out. The use of an incorrect temperature ramp creates defects during the removal of the organic vehicle. However, there are other defects which appear after the removal of the organic vehicle but they are actually related to the injection moulding stages itself. The use of compression mouldings to investigate various aspects of injection moulding, especially the origin of defects, could therefore be misleading.

Sintered test bars with a consistent density and average grain size were produced. Several sintered specimens contained micropores. However, these can be eliminated by further altering the conditions used for the removal of the organic vehicle.

Acknowledgements

The authors wish to thank CNPq of the Brazilian Government for funding given to R. Nogueira. Technical support given by Mr L. Mellet, Mr. H. Andrews and Mr K. Dutta is acknowledged. Mrs K. Goddard is thanked for typing the manuscript.

References

1. *Bull. Amer. Ceram. Soc.* **70** (1991) 1821.
2. T. ABRAHAM, *JOM*, **44** (1992) 6.
3. R. CARLSSON, *Materials Design*, **10** (1989) 10.
4. B. C. MUTSUDDY, *J. Ind. Res. Dev.* **25** (1983) 76.
5. K. SCHWARTZWALDER, *Bull. Amer. Ceram. Soc.* **28** (1949) 459.
6. M. J. EDIRISINGHE and J. R. G. EVANS, *Int. J. High Tech. Ceram.* **2** (1986) 1.
7. K. SAITO, T. TANAKA and T. HIBINO, US Patent 4 000 110, 28 December (1976).
8. S. KAMIYA, M. MURACHI, H. KAWAMOTO, S. KATO, S. KAWAKAMI and Y. SUZUKI, Publication Number 850523, Society of Automotive Engineers (SAE, Warrendale, PA, 1985).
9. M. J. EDIRISINGHE and J. R. G. EVANS, *Brit. Ceram. Trans. J.* **86** (1987) 18.
10. Y. SENO and Y. FUZITO, *Aichi-ken Kogyo Gijutsu Senta Hokoku* **24** (1988) 31.
11. M. J. EDIRISINGHE, *Ceram. Int.* **17** (1991) 89.
12. V. K. PUJARI, *J. Amer. Ceram. Soc.* **72** (1989) 10.
13. S. MASIA, P. D. CALVERT, W. E. RHINE and H. K. BOWEN, *J. Mater. Sci.* **24** (1989) 1907.
14. J. R. G. EVANS and M. J. EDIRISINGHE, *J. Mater. Sci.* **26** (1991) 2081.
15. R. E. F. Q. NOGUEIRA, M. J. EDIRISINGHE and D. T. GAWNE, *J. Mater. Sci.* in press.
16. E. A. BARRINGER and H. K. BOWEN, *J. Amer. Ceram. Soc.* **65** (1982) C199.
17. M. J. EDIRISINGHE and J. R. G. EVANS, *Indust. Ceram.* **7** (1987) 100.
18. *Idem, Proc. Brit. Ceram. Soc.* **38** (1986) 67.
19. D. R. ASHWORTH, *J. Brit. Ceram. Soc.* **6** (1969) 70.
20. ASTM Standard E112-81 (American Society for Testing and Materials, Philadelphia, PA).
21. M. I. MENDELSON, *J. Amer. Ceram. Soc.* **52** (1969) 443
22. M. O. WARMAN and D. W. BUDWORTH, *Brit. Ceram. Trans. J.* **66** (1967) 253.
23. E. DÖRRE and H. HÜBUER, in "Alumina-processing, properties and applications", edited by B. Ilschner and N. J. Grant (Springer-Verlag, Berlin, 1984) p. 58.
24. A. E. DODD, "Dictionary of ceramics" (George Newnes, London, 1967) p. 118.
25. G. S. BRADY and H. R. CLAUSER, "Materials handbook" (McGraw-Hill, New York, 1977) pp. 736–737.
26. S. A. CHAUDRI, *Polymer* **9** (1968) 604.
27. M. S. THOMAS and J. R. G. EVANS, *Brit. Ceram. Trans. J.* **87** (1988) 22–26.
28. J. G. ZHANG, M. J. EDIRISINGHE and J. R. G. EVANS, *Indust. Ceram.* **9** (1989) 72.
29. J. WOODTHORPE, M. J. EDIRISINGHE and J. R. G. EVANS, *J. Mater. Sci.* **24** (1989) 1038.
30. J. K. WRIGHT, J. R. G. EVANS and M. J. EDIRISINGHE, *J. Amer. Ceram. Soc.* **72** (1989) 1822.
31. M. J. EDIRISINGHE, *J. Mater. Sci. Lett.* **10** (1991) 1338.
32. R. H. HANSEN, in "Thermal stability of polymers", Vol 1, edited by R. T. Conley (Marcel Dekker, New York, 1970) pp. 153–187.
33. A. J. FANELLI, R. D. SILVERS, W. S. FREI, J. V. BURLEW and G. B. MARSH, *J. Amer. Ceram. Soc.* **72** (1989) 1833.
34. B. C. MUTSUDDY, *Powder Met. Int.* **19** (1987) 43.
35. R. L. COBLE, *J. Amer. Ceram. Soc.* **45** (1962) 123.
36. J. S. REED, "Introduction to the principles of ceramic processing" (John Wiley, New York, 1986) p. 459.
37. J. A. MANGELS and W. TRELA, in "Advances in ceramics", Vol. 9, edited by J. A. Mangels (American Ceramic Society, Westerville, Ohio, 1984) pp. 220–223.
38. M. F. YAN, in "Engineered materials handbook," Vol. 4, (American Society for Metals, Metals Park Ohio, 1991) pp. 270–284.
39. R. MORREL, "Handbook of properties of technical and engineering ceramics" (National Physical Laboratory, HMSO publications, London, 1987).

Received 29 June
and accepted 21 October 1992